

# L-shaped frequency selective surfaces as conducting elements on chiral slab

KEMAL DELIHACIOĞLU\*, SAVAŞ UÇKUN, TUNCAY EGE

University of Gaziantep Electrical and Electronics Engineering Department 27310 Gaziantep /Turkey

The scattering characteristics of L-shaped Frequency Selective Surfaces (FSSs) backed by chiral slab is investigated by using modal expansion method for a linearly polarized Transverse Electric (TE) incident plane wave. The Moment Method (MM) is employed by expressing the current induced on the metallic surfaces in terms of Piecewise Sinusoidal (PWS) functions. Unlike a dielectric one, chiral slab produces both co-polarized and cross-polarized fields. The variation of the co-polarized reflection and cross-polarized transmission coefficients are plotted with respect to frequency for different values of chirality admittance and oblique angle incidence. The current amplitude versus stretched out length, induced on the L-shaped FSS element is plotted at resonant frequency.

(Received May 15, 2006; accepted July 20, 2006)

*Keywords:* Chiral, L-shaped Frequency Selective Surfaces, Piecewise sinusoidal, Moment method

## 1. Introduction

Chiral materials have a great importance in electromagnetic field applications with ongoing progress. A considerable amount of experimental and analytical works have been devoted to the application of chiral materials over the last two decades [1]. Chiral materials can be used to build novel devices and structures such as, polarization transformers [2], microstrip antennas [3], chiral waveguides [4], absorbing material [5], chiro-phase shifter [6] and the reduction of target radar cross-section RCS [7]. Chiral media are known as optically active media. The special property of optically active media is that the polarization plane of linearly polarized electromagnetic wave is rotated as wave passes through the medium. The amount of rotation depends on the distance travelled by the wave in the medium and on the difference between the two wavenumbers, which is a consequence of the degree of chirality [1, 2].

Frequency Selective Surfaces (FSSs) comprised of periodically arranged metallic patch elements or aperture elements within a metallic screen exhibit total reflection or transmission. They are designed to reflect or transmit electromagnetic waves with frequency discrimination. Some applications of FSSs are band stop filters, band pass filters, microwave multiband antennas, hybrid radomes, dichroic subreflector, etc. Theoretical and experimental investigations on arrays of different FSS elements have been carried out earlier [8–11]. In antenna and microwave filter applications, periodic arrays of conducting elements are also used for Photonic Bandgap structures which prohibit the electromagnetic wave propagation within a certain frequency range [12]. The reflection and

transmission coefficients of L-shaped FSS elements on a dielectric slab were studied for the first time in [13].

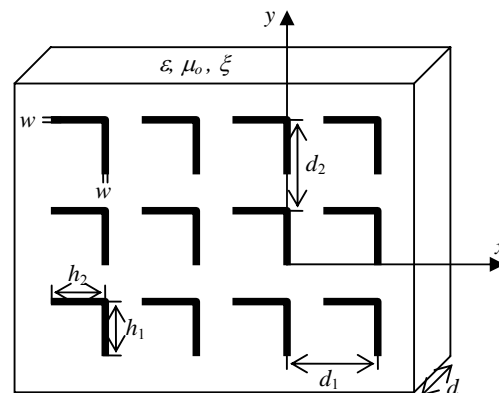


Fig. 1. L-shaped FSS conducting elements on chiral slab.

In this paper, we present a theoretical study of co-polarized reflection and cross-polarized transmission coefficients of L-shaped FSS elements on a chiral slab, as shown in Fig. 1. The improvement is the replacement of the dielectric slab with a chiral one. The current amplitude versus stretched out length, induced on the L-shaped FSS element is plotted at resonant frequency.

The FSS array is illuminated by a plane wave (TE incidence) from the free space region. The analysis is performed in the modal expansion involving Floquet [14] modes, whereby an arbitrary scattered field is represented by an infinite sum of plane waves. The incident, reflected and transmitted fields are also represented as a series of these modes. The detailed expressions for the fields in air and chiral slab can be found in [15]. The Moment Method [16] is employed by expressing the current induced on the L-shaped scatterers in terms of Piecewise Sinusoidal

(PWS) [13] functions. Since PWS basis functions are continuous within a segment, the convergence of the results is achieved by increasing the number of Floquet modes until there is little change in the results [17]. The numerical results obtained for the L-shaped FSS on chiral slab with zero chirality admittance are compared with that of L-shaped FSS on dielectric slab and proved to be excellent [13].

## 2. Theory

An isotropic, homogeneous, lossless and source free chiral medium is characterized by the following constitutive relations for electromagnetic field with time harmonic dependence, [1]

$$\mathbf{D} = \varepsilon\mathbf{E} - j\xi\mathbf{B} \quad (1)$$

$$\mathbf{H} = \frac{1}{\mu_0}\mathbf{B} - j\xi\mathbf{E} \quad (2)$$

where  $\varepsilon$ ,  $\mu_0$ , and  $\xi$ , are real values for lossless media and represent permittivity, permeability, and chirality admittance of the chiral medium, respectively. The magnitude of  $\xi$  is a measure of the degree of chirality while the sign of  $\xi$  specifies the medium handedness. A change in the sign of  $\xi$  means taking the mirror image of the material. When  $\xi > 0$ , the medium is a right handed and the sense of polarization is right handed; when  $\xi < 0$ , the medium is left handed and the sense of polarization is left handed; and when  $\xi = 0$ , the medium reduces to ordinary dielectric and there is no optical activity [2].

Inserting the constitutive relations into the source free Maxwell equations, the chiral wave equation for the electric and magnetic fields can be obtained as

$$\nabla \times \nabla \times \begin{pmatrix} \mathbf{E} \\ \mathbf{H} \end{pmatrix} - 2\omega\mu_0\xi\nabla \times \begin{pmatrix} \mathbf{E} \\ \mathbf{H} \end{pmatrix} - \omega^2\mu_0\varepsilon \begin{pmatrix} \mathbf{E} \\ \mathbf{H} \end{pmatrix} = 0 \quad (3)$$

The solution to the chiral wave equation consists of two partial waves, which are the right hand circularly (RCP) and left hand circularly polarized (LCP) waves, inside the chiral medium.

$$k_R = \omega\mu_0\xi + \sqrt{\omega^2\mu_0^2\varepsilon^2 + k^2} \quad (4)$$

$$k_L = -\omega\mu_0\xi + \sqrt{\omega^2\mu_0^2\varepsilon^2 + k^2} \quad (5)$$

with  $k_R$  corresponding to RCP and  $k_L$  to the LCP wave. When  $\xi = 0$ . The two characteristic waves propagate at different velocities in a medium, which is called birefringence.

L-shaped FSS elements, consisting of an infinitely thin and perfect conductor, are placed periodically on the x-y plane, as shown in Fig. 1. Due to the periodicity of the problem, the fields are expanded into Floquet modes in the air and chiral regions. The incident electric field will induce currents on FSS elements which in turn will be scattered in the forward and backward directions. The

amplitude of the scattered fields can be expressed in terms of the induced current density on the conducting elements of L-shaped by using the appropriate boundary conditions [13]. Finally, an Electric Field Integral Equation (EFIE) is obtained by imposing the total electric field to be zero over the conducting area of a single periodic unit cell. Substituting basis functions into the EFIE and then integrating it over a unit cell using the Galerkin method, the EFIE is finally transformed into a complex matrix equation. The dimension of the matrix is equal to the number of basis functions used. The unknown current coefficients are then computed using matrix inversion techniques. Having computed the current coefficients, the co-polarized reflected and cross-polarized transmitted waves can readily be found.

## 3. Numerical results and discussion

The magnitude of co-polarized reflection and cross-polarized transmission coefficients are plotted against frequency for different values of chirality admittances and oblique incident angles. The amplitude of the induced current is plotted with respect to total length of the L-shaped FSS structure. Four coefficients are calculated for a chiral slab for TE incidence. That is, two reflection and two transmission coefficients. For TE incidence the cross-polarized wave is a TM one. The reflection coefficient for a cross-polarized wave and the transmission coefficient for a co-polarized wave are not plotted. When the chirality admittance is set equal to zero ( $\xi = 0$ ), the chiral slab becomes equivalent to a dielectric slab. The numerical results are compared with L-shaped FSS elements on a dielectric slab of 0.1 cm thickness and same results are obtained as in [13]. The validity of the formulation is also ensured by comparing the numerical results with that in [15] given for narrow strip FSSs backed by a chiral slab and proved to be as good. The convergence of the results is obtained by increasing the number of Floquet modes until there is little change in the results. The number of Floquet modes used is  $(2p+1)^2$ , where  $p=9$ . The only propagating mode is the zero order Floquet mode, which is the fundamental one. All other modes are evanescent or decaying. The lengths of L-shaped FSS elements are  $h_1=h_2=0.9$  cm and the width is  $w=0.09$  cm. The chiral slab thickness ( $d$ ) and dielectric constant ( $\varepsilon_r$ ) are 0.5 cm and 1.6, respectively. The periodic cells are arranged in a square lattice where the unit cell dimensions are  $d_1=d_2=0.93$  cm. The number of basis functions used to estimate the current coefficients for L-shaped FSS are 19. The value of chirality admittance is varied in the range given by the inequality  $|\xi| \leq \sqrt{\varepsilon_r\varepsilon_0/\mu_0}$  [18].

Fig. 2. illustrates the variations of co-polarized reflection ( $R_{co}^{TE}$ ) and cross-polarized transmission ( $T_{cr}^{TM}$ ) coefficients as a function of frequency for different values of  $\xi$  at normal incidence. In Fig. 2a. there is only one resonance frequency (total reflection) for the chirality admittances of  $\xi=0$  and  $\xi=0.001$  mho. Further increase in chirality admittance results in multiple resonances. At 10 GHz the magnitude of co-polarized reflection

coefficient is nearly the same for different values of  $\xi$ . As can be seen from Fig. 2a, at low chirality admittance the magnitudes of co-polarized reflection is very close to the reflection coefficient of dielectric backed L-shaped FSSs. As shown in Fig. 2b, the cross-polarized transmission coefficient has nulls at resonance frequencies. There is a full transmission (anti-resonance) for the cross-polarized wave at  $\xi=0.002$  and  $\xi=0.003$  mho, which means that the polarization state of the incident TE wave is converted to TM wave at that frequency. The polarization conversion is caused by optical activity, as expected from chiral slab.

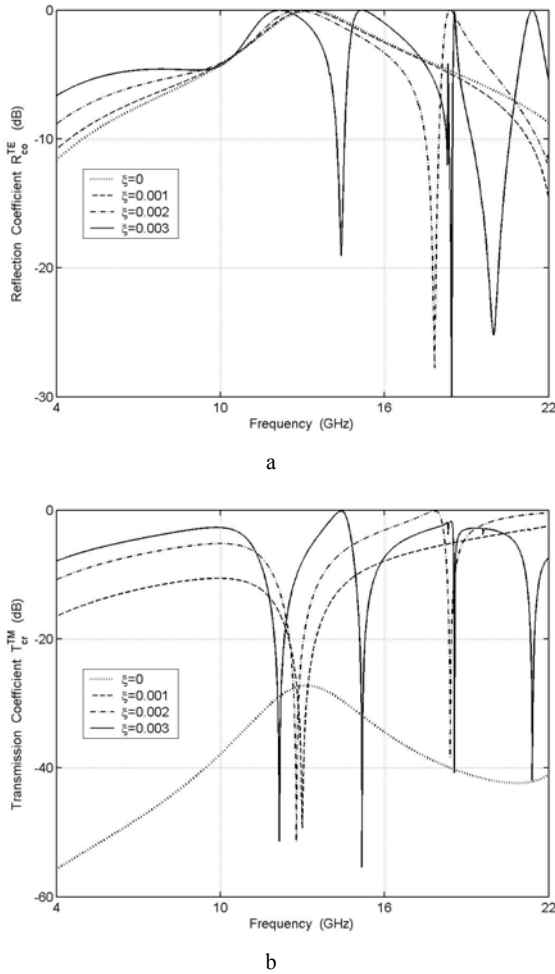


Fig. 2. Reflection and transmission coefficients of L-shaped FSS on a chiral slab for different chirality admittances; TE incidence,  $\theta=\phi=0^\circ$ ,  $d=0.5$  cm,  $\epsilon_r=1.6$ ,  $w=0.09$  cm,  $h_1=h_2=0.9$  cm,  $d_1=d_2=0.93$  cm, (a) Reflection coefficient  $R_{co}^{TE}$ , (b) Transmission coefficient  $T_{cr}^{TM}$ .

Fig. 3 shows the variation of co-polarized reflection and cross-polarized transmission coefficients versus frequency as the angle of incidence changes. As shown in Fig. 3a, two resonance frequencies are seen at normal incidence. The magnitude of co-polarized reflection

coefficient is very close to unity around 12 GHz for oblique incidence angle variations. The second resonance seen at normal incidence disappears for an obliquely incident wave. As seen in Fig. 3b, the polarization conversions occur at different frequencies for normal and oblique angle of incidences.

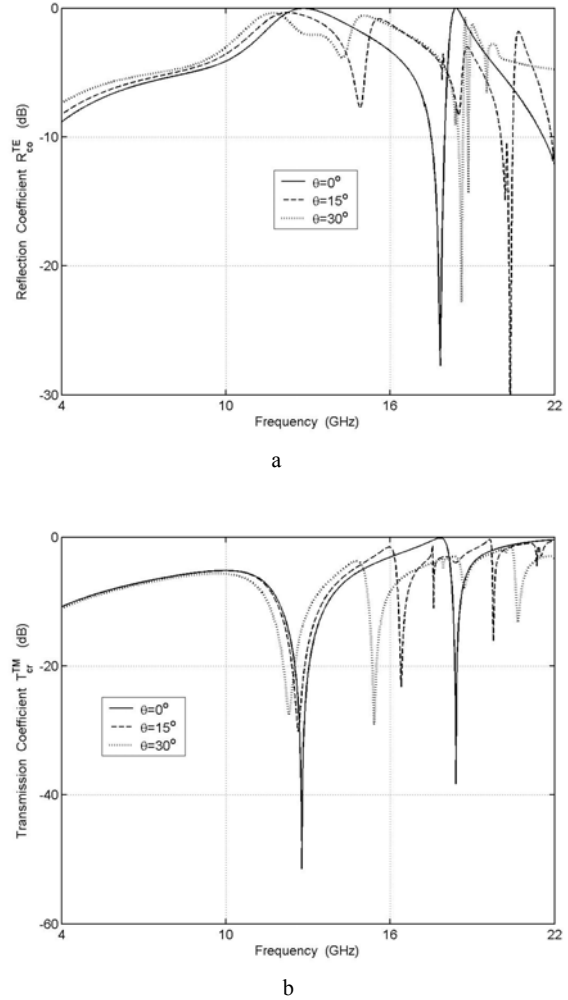


Fig. 3. Reflection and transmission coefficients of L-shaped FSS on a chiral slab for different incident angles; TE incidence,  $\phi=0^\circ$ ,  $\xi=0.002$  S,  $d=0.5$  cm,  $\epsilon_r=1.6$ ,  $w=0.09$  cm,  $h_1=h_2=0.9$  cm,  $d_1=d_2=0.93$  cm, (a) Reflection Coefficient  $R_{co}^{TE}$ , (b) Transmission Coefficient  $T_{cr}^{TM}$ .

Fig. 4 illustrates the current amplitude versus stretched out length, induced on the L-shape FSS elements backed by chiral slab, at resonant frequencies ( $f_r$ ) for  $\xi=0.002$  mho. The resonant frequencies are at 12.85 and 18.4 GHz for  $\xi=0.002$  mho. For an array consisting of conducting elements under plane wave incidence, a maximum current magnitude is excited on the elements at the array resonant frequency. The current in this case is in phase with the incident field, i.e., the impedance seen by

the incident wave is purely ohmic (real), since the capacitive and inductive parts cancel out. As a result of the resonance, the incident wave is reflected with a phase reversal. The incident electric field, which is in  $a_y$  direction with a unity amplitude, induces more current in the parallel arm while it induces less current in the perpendicular arm of the L-shape FSS.

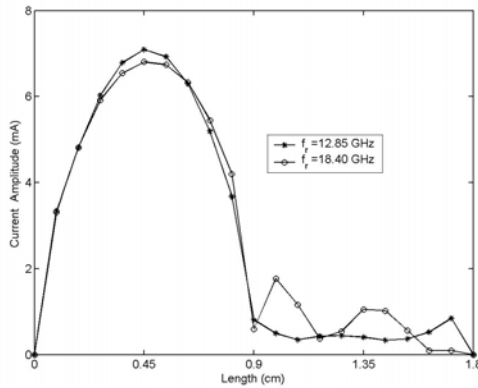


Fig. 4. Current amplitude versus length at resonance frequencies of L-shape FSS on a chiral slab;  $\theta = \phi = 0^\circ$ ,  $\xi = 0.002$  S,  $d = 0.5$  cm,  $\epsilon_r = 1.6$ ,  $w = 0.09$  cm,  $h_1 = h_2 = 0.9$  cm,  $d_1 = d_2 = 0.93$  cm.

#### 4. Conclusions

L-shaped FSS elements on chiral slab are analyzed for a TE incident plane wave. The co-polarized reflection and cross-polarized transmission coefficients are plotted against frequency for various chirality admittances and incident angles. The current versus stretched out length is plotted at two different resonant frequencies for  $\xi = 0.002$ . Numerical results illustrate that the chirality admittance of the slab causes a significant polarization rotation. At  $\xi = 0.002$  and  $\xi = 0.003$  mho values, there is a full transmissions (anti-resonances) for the cross-polarized wave at normal incidence, which states the polarization conversion. Polarization conversion is also observed at an angle of  $15^\circ$  for an obliquely incident wave. Multiple resonances occur for high values of chirality admittance. The results of L-shaped FSS on chiral slab can be used as multiple band stop filter application at different frequency regions.

#### References

- [1] I. V. Lindell, A. H. Sihvola, S. A. Tretyakov, A. J. Viitanen, *Electromagnetic Waves in Chiral and Bi-Isotropic Media*, Norwood, MA (1994).
- [2] S. Bassiri, C. H. Papas, N. Engheta *J. Opt. Soc. Am. A* **5**, 1450 (1988).
- [3] D. Pozar, *IEEE Trans. Antennas Propagat.* **40**, 1260 (1992).
- [4] P. Pelet, N. Enghata, *IEEE Trans. Antennas Propagat.* **38**, 90 (1990).
- [5] A. M. M. Allam 17-th National Radio Science Conference, Minufiya University, Egypt, 2000.
- [6] M. I. Mamdouh, N. Engheta, *IEEE Trans. Microw. Theory & Tech.* **42**, 1690 (1994).
- [7] D. L. Jaggard, N. Enghata, *Elec. Letters* **25**, 173 (1989).
- [8] B. A. Munk, *Frequency Selective Surfaces: Theory and Design*, Wiley, New York (2000).
- [9] J. C. Vardaxoglou, *Frequency Selective Surfaces: Analysis and Design*, Wiley, New York (1997).
- [10] R. Mittra, C. H. Chan, T. Cwik, *IEEE Proceedings*, **76**, 1593 (1988).
- [11] C. H. Tsao, R. Mittra, *IEEE Trans. Antennas Propagat.* **32**, 478 (1984).
- [12] Y. L. R. Lee, A. Chauraya, D. S. Lockyer, J. C. Vardaxoglou, *IEE Proc. Optoelectron.* **147**, 395 (2000).
- [13] K. Delihacioglu, S. Uçkun, T. Ege, Scattering characteristics of FSS comprised of L-shaped and one-turn helix shaped conductors for TE and TM excitation. *Electr. Eng.* (accepted for publication).
- [14] N. Amitay, V. Galindo, C. P. Wu, *Theory and analysis of phased array antennas*, Wiley-Interscience, New York (1972).
- [15] A. O. Koca, *Analysis of Frequency Selective Surfaces on Chiral Slab*, PhD Dissertation, University of Gaziantep (1997).
- [16] R. F. Harrington, *Field computation by moment methods*, MacMillan, New York (1968).
- [17] K. J. Webb, P. W. Grounds, R. Mittra, *IEEE Trans Antennas Propagat.* **38**, 869 (1990).
- [18] N. Engheta, D. L. Jaggard, *IEEE AP-S Newslett.* **30**, 6 (1988).

\*Corresponding author: kemal@gantep.edu.tr